
**Liquid Crystals**
Publication details, including instructions for authors and subscription information:
http://www.informaworld.com/smpp/title~content=t713926090

# Synthesis, thermal stabilities, and anisotropic properties of some new isoflavone-based esters 7-decanoyloxy-3-(4'-substitutedphenyl)-4H-1-benzopyran-4-ones

Guan-Yeow Yeap[a]; Wan-Sinn Yam[a]; Daisuke Takeuchi[b]; Kohtaro Osakada[b]; Ewa Gorecka[c]; Wan Ahmad Kamil Mahmood[a]; Peng-Lim Boey[a]; Shafida Abd Hamid[a]
[a] Liquid Crystal Research Laboratory, School of Chemical Sciences, Universiti Sains Malaysia, 11800 Minden, Penang, Malaysia [b] Chemical Resources Laboratory (Mail Box R1-03), Tokyo Institute of Technology, 4259 Nagatsuta, Midori-ku, Yokohama, 226-8503, Japan [c] Department of Chemistry, Warsaw University, 02-089 Warsaw, Poland

**To cite this Article** Yeap, Guan-Yeow , Yam, Wan-Sinn , Takeuchi, Daisuke , Osakada, Kohtaro , Gorecka, Ewa , Mahmood, Wan Ahmad Kamil , Boey, Peng-Lim and Hamid, Shafida Abd(2008) 'Synthesis, thermal stabilities, and anisotropic properties of some new isoflavone-based esters 7-decanoyloxy-3-(4'-substitutedphenyl)-4H-1-benzopyran-4-ones', Liquid Crystals, 35: 3, 315 — 323
**To link to this Article: DOI:** 10.1080/02678290701875811
**URL:** http://dx.doi.org/10.1080/02678290701875811

*Liquid Crystals,*
Vol. 35, No. 3, March 2008, 315–323

Taylor & Francis
Taylor & Francis Group

# Synthesis, thermal stabilities, and anisotropic properties of some new isoflavone-based esters 7-decanoyloxy-3-(4′-substitutedphenyl)-4H-1-benzopyran-4-ones

Guan-Yeow Yeap[a]*, Wan-Sinn Yam[a], Daisuke Takeuchi[b], Kohtaro Osakada[b], Ewa Gorecka[c], Wan Ahmad Kamil Mahmood[a], Peng-Lim Boey[a] and Shafida Abd Hamid[a]

[a]*Liquid Crystal Research Laboratory, School of Chemical Sciences, Universiti Sains Malaysia, 11800 Minden, Penang, Malaysia;* [b]*Chemical Resources Laboratory (Mail Box R1-03), Tokyo Institute of Technology, 4259 Nagatsuta, Midori-ku, Yokohama, 226-8503, Japan;* [c]*Department of Chemistry, Warsaw University, Al.Zwirki I Wigury 101, 02-089 Warsaw, Poland*

*(Received 3 April 2007; final form 12 December 2007)*

A series of new isoflavonic esters 7-decanoyloxy-3-(4′-substitutedphenyl)-4H-1-benzopyran-4-ones containing a heterocycle in their central core with one flexible alkyl chain and various substituents, R (where R=F, Cl, Br, $CH_3$, $OCH_3$, or H) at 4′-position at one end, have successfully been synthesised, isolated, and characterised. The physical properties of title compounds were studied using spectroscopic techniques (Fourier transform infrared, $^1H$ and $^{13}C$ nuclear magnetic resonance). The liquid crystalline properties and the textures of these compounds along with their thermal stabilities were investigated via polarising optical microscopy and differential scanning calorimetry. All the compounds except the member without the substituent were enantiotropic mesogens exhibiting smectic A and/or nematic phases. The layer periodicities in relation to different phases were substantiated by X-ray diffraction wherein the molecules within the SmA phase were found to be intercalated. The structural changes that resulted in a variation of transition temperature as well as the electronic polarisability of the respective compounds are also discussed.

**Keywords:** heterocycle; 7-decanoyloxy-3-(4′-substitutedphenyl)-4H-1-benzopyran-4-ones; enantiotropic mesogens; nematic; smectic A; thermal stabilities



## 1. Introduction

It has been well established that the compounds with a classical rod-like structure constructed from the conjugated aromatic central core with one or two flexible terminal chains exhibit liquid crystalline properties. The growing scientific interest on the synthesis of these compounds has continued to develop up to the present today. One of the typical classes of compounds exhibiting liquid crystalline behaviour is those with heterocyclic rings such as isoflavones in their central cores (*1–3*). In our previous report, we observed the correlation between the phase behaviour with both the molecular structure and the presence of a lateral dipole associated with the intermolecular interaction within the mesophase (*4*). In our present study, we synthesised and characterised the analogous compounds incorporating similar isoflavonic moiety within the central core. However, in this series, one of the terminal ends along the long molecular axis is attached with different substituents. The influence of these substituents on the mesomorphic properties of the title compounds is reported in this article. These novel compounds include 7-decanoyloxy-3-(4′-substitutedphenyl)-4H-1-benzopyran-4-ones in which the substituent R is F, Cl, Br, $CH_3$, $OCH_3$, or H. While the elemental analysis, Fourier transform infrared (FT-IR), $^1H$, and $^{13}C$ nuclear magnetic resonance (NMR) spectroscopic studies support the proposed structure, the mesomorphic properties of the title compounds were studied explicitly using a polarising optical microscope (POM) and differential scanning calorimetry (DSC). The molecular packing within the mesomorphic region was demonstrated further by X-ray diffraction.

## 2. Experimental

### 2.1. *Reagents and synthetic methods*

Resorcinol (Aldrich), methanesulfonyl chloride, boron trifluoride (Merck), decanoyl chloride (Acros), phenylacetic acid, and its *p*-substituted analogues (*p*-fluoro-, *p*-chloro-, *p*-bromo-, *p*-nitro-, *p*-tolyl-, and *p*-methoxyphenylacetic acids (TCI, Japan)) were used without further purification. Thin-layer chromatography was performed using aluminium-backed silica-gel plates (Merck 60 F254), which were examined under UV light. Column chromatography was performed using Merck 60-mesh silica gel.

Microanalyses for all compounds were carried out by a 2400 LS series CHNS/O analyser. The IR spectra were recorded on a Perkin Elmer 2000-FTIR spectrophotometer in a frequency range of

*Corresponding author. Email: gyyeap@usm.my or gyyeap_liqcryst_usm@yahoo.com

ISSN 0267-8292 print/ISSN 1366-5855 online

DOI: 10.1080/02678290701875811
http://www.informaworld.com

4000–400 $cm^{-1}$ in which the samples were embedded in KBr discs. NMR data were obtained using Bruker 300-MHz and 400-MHz ultrashied spectrometer equipped with a 5-mm broad band inverse (BBI) gradient probe, respectively. A standard Bruker pulse program (*5*) was used throughout the experiment. Complete $^{1}H$ and $^{13}C$ NMR assignment of representative compounds were obtained and substantiated by means of $^{1}H$-$^{1}H$ correlation spectroscopy (COSY), $^{12}C$–$^{1}H$ heteronuclear multiple quantum correlation (HMQC), and $^{13}C$–$^{1}H$ heteronuclear multiple bond correlation (HMBC) spectroscopic measurements, as described in the literature (*6, 7*). Deuterated chloroform ($CDCl_3$), acetone-$d_6$, and dimethylsulphoxide (DMSO-$d_6$) were used as solvents and TMS as internal standard. The phase transition temperatures and enthalpy values were recorded by Seiko DSC6200R differential scanning calorimetry at heating and cooling rates of 5°C $min^{-1}$ and −5°C $min^{-1}$, respectively. The textures of the mesophases were studied using a Carl Zeiss polarising microscope with a Linkam LTS350 hot stage and temperature controller attached. The samples studied by optical microscopy were prepared as a thin film sandwiched between glass slide and cover. The thermal behaviour was studied based on the enthalpy values expressed in $kJmol^{-1}$.

A Bruker D8 diffractometer (CuK$\alpha$=1.54 Å) with a Vantec detector was used to measure the layer spacing of the compound with methyl substituent. A glass slide containing a thin layer of this compound was placed on a heating stage and orientated homeotropically. The quality of alignment was ensured by rocking scans with a rocking curve width of 1–2°. The temperature step was 1 K with stability better than 0.1 K. All measurements are performed with a reflection mode in parallel beam geometry obtained with a Göbel mirror.

A molecular modelling study was performed using ACD/Chemsketch Version 4.5. Geometrical optimisation or energy minimisation of the molecules was carried out to reveal the molecular shape and geometry. The structural conformation obtained was subsequently used to calculate the polarisability of each compound.

## 2.2. *Synthesis*

The synthesis of the intermediates **1**–**12** and the ultimate compounds **13**–**18** were carried out using the experimental procedure, as described in Scheme 1.

### *2.2.1. Synthesis of 1-(2,4-dihydroxyphenyl)-2-(4′-substitutedphenyl)-ethanone, 1–6.*

A mixture containing 5 g of the appropriate 4-substituted phenylacetic acid and 1.0 equiv of resorcinol in 40 ml $BF_3.Et_2O$ was heated for 4 h at 70–75°C under nitrogen atmosphere (*8*). The mixture was cooled down to ambient temperature and poured into an ice-water bath. The oil was separated, air-dried, and recrystallised from chloroform.

### *2.2.2. Synthesis of 7-hydroxy-3-(4′-substitutedphenyl)-4H-1-benzopyran-4-one, 7–12.*

5 g of 1-(2,4-dihydroxyphenyl)-2-(4-substitutedphenyl)ethanone in dry dimethylformamide (DMF) was carefully treated with 4.0 equiv of $BF_3$•$Et_2O$ under nitrogen atmosphere. To this mixture, 3.0 equiv of $MeSO_2Cl$ was added at 50–55°C and stirred for 1 h. The mixture was then heated for 1.5 h at 75–80°C (*9, 10*) prior to being poured with rapid stirring into an ice-water bath. The product thus obtained was subsequently purified with chloroform.

### *2.2.3. Synthesis of 7-decanoyloxy-3-(4′-substitutedphenyl)-4H-1-benzopyran-4-one, 13–18.*

1.2 equiv of decanoylchloride was added to a mixture of 0.3 g 7-hydroxy-3-(4-substitutedphenyl)-4H-1-benzopyran-4-one in DMF/$CH_2Cl_2$ and 0.2 ml triethylamine. The mixture was stirred at room temperature for 6 h. The solvent was later removed and diethylether was added to the residue. Triethylamonium chloride was filtered off and the product was purified using column chromatography with chloroform/ethyl acetate 9:1 as eluent. The compounds were further purified through recrystallisation from absolute ethanol.

All the compounds thus synthesised were characterised by spectroscopic techniques, as stated in the earlier section. The analytical results obtained were summarised as follows:

**1**: Yield 65%. Melting point (m.p.) 140.0–141.0°C. Analysis: calculated for $C_{14}H_{11}FO_3$. C 68.29, H 4.50%; found C 68.10%, H 4.48%. IR (KBr)/$cm^{-1}$: 3419 (OH), 2907 ($CH_2$ aliphatic), 1636 (C=O), 1598 (C=C). $^{1}H$ NMR (acetone-$d_6$) $\delta$/ppm: 12.65 (1H, s, OH), 9.58 (1H, s, OH), 6.34–7.96 (7H, Ar–H), 4.33 (2H, s, $CH_2$). $^{13}C$ NMR (acetone-$d_6$) $\delta$/ppm: 202.56 (C=O), 166.14, 165.31, 136.76, 133.61, 131.88, 131.77, 115.42, 113.02, 108.55, 103.27 ($C_{arom}$), and 43.54 ($CH_2$).

**2**: Yield 63%. m.p. 150.0–150.5°C. Analysis: calculated for $C_{14}H_{11}ClO_3$. C 64.01, H 4.22%; found C 64.02, H 4.23%. IR (KBr)/$cm^{-1}$: 3358 (OH), 2920 ($CH_2$ aliphatic), 1630 (C=O), 1596 (C=C). $^{1}H$ NMR (acetone-$d_6$) $\delta$/ppm: 12.62 (1H, s, OH), 9.62 (1H, s, OH), 6.34–7.89 (7H, Ar–H), 4.35 (2H, s, $CH_2$). $^{13}C$ NMR (acetone-$d_6$) $\delta$/ppm: 202.26 (CO), 166.11, 165.53, 134.60, 133.60, 131.77, 131.54, 128.75, 112.90, 108.56, 103.15 ($C_{arom}$), and 43.67 ($CH_2$).

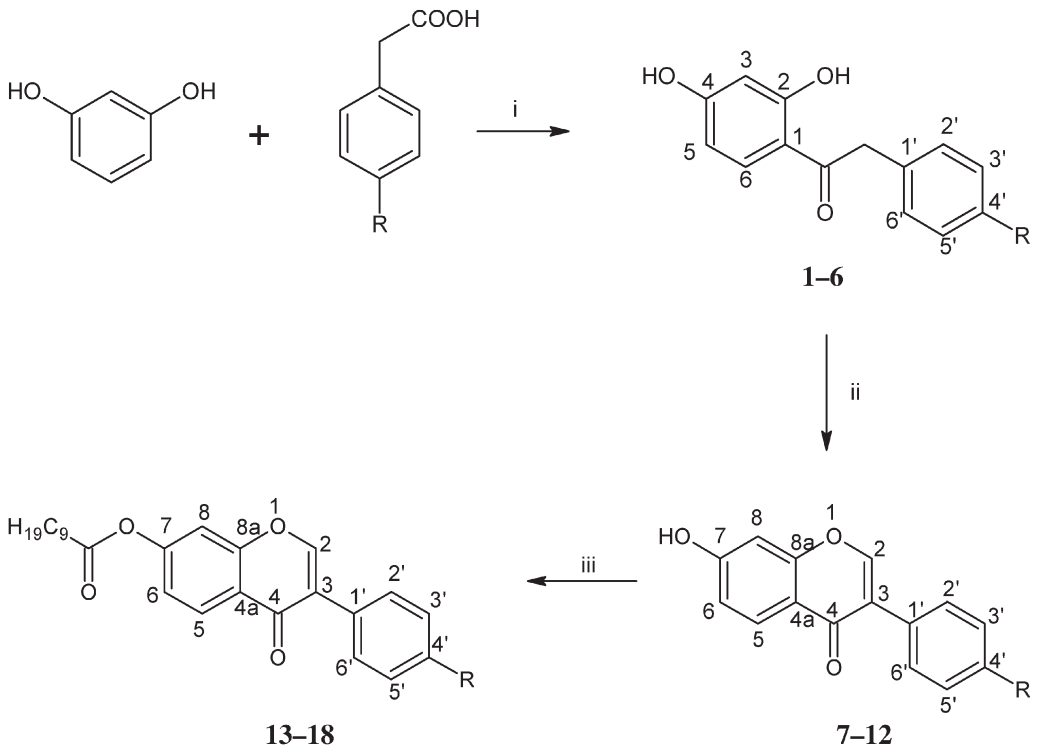


| Compound | R |
|---|---|
| **13** | F |
| **14** | Cl |
| **15** | Br |
| **16** | $CH_3$ |
| **17** | $OCH_3$ |
| **18** | H |

Scheme 1. Synthetic route towards the formation of intermediates and title compounds **1**–**18**. Reagents and conditions: (i) $BF_3/Et_2O$ heat at 70–75°C for 4 h; (ii) $N_2$ atmosphere, DMF, $BF_3/Et_2O$ heat at 55°C for 1 h; $MeSO_2Cl$ heat for 1.5 h; (iii) $N_2$ atmosphere, DMF, $CH_2Cl_2$, $(C_2H_5)_3N$, stir at room temperature for 6 h.

**3**: Yield 68%. m.p. 170.0–170.5°C. Analysis: calculated for $C_{14}H_{11}BrO_3$. C 57.75, H 3.61%; found C 57.65, H 3.60%. IR (KBr)/$cm^{-1}$: 3322 (OH), 2892 ($CH_2$ aliphatic), 1626 (C=O), 1587 (C=C). $^1$H NMR (acetone-$d_6$) $\delta$/ppm: 12.62 (1H, s, OH), 9.60 (1H, s, OH), 6.34–7.99 (7H, Ar–H), 4.35 (2H, s, $CH_2$). $^{13}$C NMR (acetone-$d_6$) $\delta$/ppm: 204.18 (CO), 166.15, 165.28, 135.07, 133.60, 132.10, 131.75, 120.58, 113.08, 108.47, 103.20 ($C_{arom}$), and 43.77 ($CH_2$).

**4**: Yield 69%. m.p. 144.0–145.0°C. Analysis: calculated for $C_{15}H_{14}O_3$. C 74.36%, H 5.82%; found C 74.16, H 5.80%. IR (KBr)/$cm^{-1}$: 3145 (OH), 2922, 2870 ($CH_2$ aliphatic), 1623 (C=O), 1584 (C=C). $^1$H NMR (acetone-$d_6$) $\delta$/ppm: 12.74 (1H, s, OH), 9.56 (1H, s, OH), 6.32–7.97 (7H, Ar–H), 4.24 (2H, s, $CH_2$), 2.28 (3H, s, $CH_3$). $^{13}$C NMR (acetone-$d_6$) $\delta$/ppm: 205.53 (CO), 166.24, 165.24, 136.50, 133.83, 132.63, 129.66, 129.48, 112.99, 108.39, 103.15 ($C_{arom}$), 44.25 ($\underline{C}H_2$–CO), and 20.51(Ar–$CH_3$).

**5**: Yield 60%. m.p. 156.0–157.0°C. Analysis: calculated for $C_{15}H_{14}O_4$. C 69.76, H 5.46%; found C 69.50, H 5.43%. IR (KBr)/$cm^{-1}$: 3412 (OH), 2836 ($CH_2$ aliphatic), 1631 (C=O), 1568 (C=C), 1244 (C–O). $^1$H NMR (acetone-$d_6$) $\delta$/ppm: 12.75 (1H, s, OH), 9.58 (1H, s, OH), 6.32–7.98 (7H, Ar–H), 4.23 (2H, s, $CH_2$), 3.77 (3H, s, $OCH_3$). $^{13}$C NMR (acetone-$d_6$) $\delta$/ppm: 205.49 (CO), 166.23, 165.15, 159.11, 133.81, 130.80, 127.46, 114.26, 112.97, 108.35, 103.16 ($C_{arom}$), 54.96 ($OCH_3$), and 43.72 ($CH_2$).

**6**: Yield 63%. m.p. 138.0–139.0°C. Analysis: calculated for $C_{14}H_{12}O_3$. C 73.07, H 5.30%; found C 73.20, H 5.32%. IR (KBr)/$cm^{-1}$: 3212 (OH), 2900 ($CH_2$ aliphatic), 1639 (C=O), 1549 (C=C). $^1$H NMR (acetone-$d_6$) $\delta$/ppm: 12.72 (1-H, s, OH), 9.58 (1H, s, OH), 6.34–7.98 (7H, Ar–H), 4.30 (2H, s, $CH_2$). $^{13}$C

NMR (acetone-$d_6$) $\delta$/ppm: 202.84 (CO), 166.22, 165.26, 135.71, 133.81, 129.85, 128.84, 127.26, 113.16, 108.44, 103.20 ($C_{arom}$), and 44.59 ($CH_2$).

**7**: Yield 59%. m.p.202.0–203.0°C. Analysis: calculated for $C_{15}H_9FO_3$. C 70.31, H 3.54%; found C 70.42, H 3.55%. IR (KBr)/$cm^{-1}$: 3193 (OH), 1641 (C=O), 1598 (C=C). $^1$H NMR (DMSO-$d_6$) $\delta$/ppm: 10.85 (1H, s, OH), 8.41 (1H, s, H), 6.89–7.99 (7H, Ar–H). $^{13}$C NMR (DMSO-$d_6$) $\delta$/ppm: 174.28 (CO), 162.65, 157.40, 153.75, 130.92, 130.81, 127.20, 122.48, 116.45, 115.24, 115.02, 114.74, 102.11 ppm ($C_{arom}$).

**8**: Yield 60%. m.p. 229.0–230.0°C. Analysis: calculated for $C_{15}H_9ClO_3$. C 66.07, H 3.33%; found C 66.00, H 3.33%. IR (KBr)/$cm^{-1}$: 3197 (OH), 1642 (C=O), 1593 (C=C). $^1$H NMR (DMSO-$d_6$) $\delta$/ppm: 10.98 (1H, s, OH), 8.52 (1H, s, Ar–H), 6.99–8.09 (7H, Ar–H). $^{13}$C NMR (DMSO-$d_6$) $\delta$/ppm: 175.09 (CO), 163.64, 154.96, 128.32, 133.34, 131.85, 131.51, 128.98, 128.16, 123.19, 117.36, 116.25, and 103.08 ($C_{arom}$).

**9**: Yield 63%. m.p. 242.0–243.0°C. Analysis: calculated for $C_{15}H_9BrO_3$. C 56.81, H 2.86%; found C 56.70, H 2.83%. IR (KBr)/$cm^{-1}$: 3177 (OH), 1641 (C=O), 1588 (C=C). $^1$H NMR (DMSO-$d_6$) $\delta$/ppm: 10.96 (1H, s, OH), 8.54 (1H, s, Ar–H), 6.99–8.09 (7H, Ar–H). $^{13}$C NMR (DMSO-$d_6$) $\delta$/ppm: 175.03 (CO), 163.64, 158.34, 154.87, 132.27, 131.90, 131.82, 128.16, 123.28, 121.92, 117.42, 116.25, and 103.09 ($C_{arom}$).

**10**: Yield 70%. m.p. 254.0–255.0°C. Analysis: calculated for $C_{16}H_{12}O_3$. C 76.18, H 4.74%; found C 76.30, H 4.75%. IR (KBr)/$cm^{-1}$: 3188 (OH), 1623 (C=O), 1574 (C=C). $^1$H NMR (DMSO-$d_6$) $\delta$/ppm: 10.85 (1H, s, OH), 8.41 (1H, s, Ar–H), 6.89–7.99 (7H, Ar–H), 3.48 (3H, s, $CH_3$). $^{13}$C NMR (DMSO-$d_6$) $\delta$/ppm: 175.36 (CO), 163.47, 158.30, 154.33, 137.87, 130.01, 129.61, 129.54, 128.16, 124.30, 117.50, 116.08, 103.01 ($C_{arom}$), and 21.66 ($CH_3$).

**11**: Yield 55%. m.p. 217.0–218.0°C. Analysis: calculated for $C_{16}H_{12}O_4$. C 71.64, H 4.51%; found C 71.68, H 4.52%. IR (KBr)/$cm^{-1}$: 3137 (OH), 1638 (C=O), 1595 (C=C), 1246 (C–O). $^1$H NMR (DMSO-$d_6$) $\delta$/ppm: 10.90 (1H, s, OH), 8.43 (1H, s, Ar–H), 6.97–8.08 (7H, Ar–H), 3.45 (3H, s, $OCH_3$). $^{13}$C NMR (DMSO-$d_6$) $\delta$/ppm: 175.46 (CO), 163.42, 159.81, 158.30, 153.96, 130.92, 128.14, 125.11, 124.02, 117.49, 116.03, 114.44, 102.98 ($C_{arom}$), and 55.98 ($OCH_3$).

**12**: Yield 61%. 199.5–200.0°C. Analysis: calculated for $C_{15}H_{10}O_3$. C 75.62, H 4.23%; found C 75.80, H 4.30%. IR (KBr)/$cm^{-1}$: 3200 (OH), 1622 (C=O), 1584 (C=C). $^1$H NMR (DMSO-$d_6$) $\delta$/ppm: 10.85 (1H, s, OH), 8.41 (1H, s, Ar–H), 6.89–7.99 (7H, Ar–H). $^{13}$C NMR (DMSO-$d_6$) $\delta$/ppm: 174.76 (CO), 163.03, 157.83, 154.17, 132.49, 129.30, 128.46, 128.08, 127.68, 123.92, 117.05, 115.63, 102.54 ($C_{arom}$).

**13**: Yield 50%. Analysis: calculated for $C_{25}H_{27}FO_4$. C 73.15, H 6.63%; found C 73.00, H 6.60%. IR (KBr)/$cm^{-1}$: 2959, 2916, 2851 ($CH_2$ aliphatic), 1754 (C=O ester), 1637 (C=O pyranone), 1609 (C=C). $^1$H NMR ($CDCl_3$) $\delta$/ppm: 8.32 (1H, d, Ar–H), 7.99 (1H, s, Ar–H), 7.31 (1H, d, Ar–H), 7.11–7.18 (3H, dd, Ar–H), 7.12 (2H, d, Ar–H), 2.59–2.63 (2H, t, $CH_2COO$), 1.74–1.82 (2H, m, $C\underline{H}_2$–$CH_2COO$), 1.29–1.45 (12H, m, $CH_3(C\underline{H}_2)_6$–$C_2H_4COO$), 0.87–0.91 (3H, t, $CH_3$). $^{13}$C NMR ($CDCl_3$) $\delta$/ppm: 175.73 (C=O pyranone), 171.84 (C=O ester), 157.06, 155.17, 153.50, 134.77, 130.61, 130.41, 129.15, 128.20, 124.93, 120.14, 115.55, 111.35 ($C_{arom}$), 34.80, 32.25, 29.80, 29.64, 29.47, 25.19, 23.07, and 14.50 ($\underline{C}_9H_{19}COO$–).

**14**: Yield 45%. Analysis: calculated for $C_{25}H_{27}ClO_4$. C 70.33, H 6.37%; found C 70.13, H 6.33%. IR (KBr)/$cm^{-1}$: 2952, 2928, 2855 ($CH_2$ aliphatic), 1745 (C=O ester), 1647 (C=O pyranone), 1576 (C=C). $^1$H NMR ($CDCl_3$) $\delta$/ppm: 8.31 (1H, d, Ar–H), 8.00 (1H, s, H-2), 7.50 (2H, d, Ar–H), 7.41 (2H, d, Ar–H), 7.30 (1H, d, Ar–H), 7.15–7.18 (1H, dd, Ar–H), 2.59–2.63 (2H, t, $CH_2COO$), 1.69–1.79 (2H, m, $C\underline{H}_2$–$CH_2COO$), 1.29–1.44 (12H, m, $CH_3(C\underline{H}_2)_6$–$C_2H_4COO$), 0.87–0.91 (3H, t, $CH_3$). $^{13}$C NMR ($CDCl_3$) $\delta$/ppm: 175.53 (C=O pyranone), 171.46 (C=O ester), 156.70, 154.74, 152.97, 130.76, 130.41, 130.66, 127.81, 127.47, 124.72, 122.17, 119.69, 110.95 ($C_{arom}$), 34.42, 31.86, 29.41, 29.25, 29.08, 24.81, 22.68, 14.11 ($\underline{C}_9H_{19}COO$–).

**15**: Yield 50%. Analysis: calculated for $C_{25}H_{27}BrO_4$. C 63.70, H 5.77%; found C 62.95, H 5.57%. IR (KBr)/$cm^{-1}$: 2953, 2925, 2853 ($CH_2$ aliphatic), 1742 (C=O ester), 1648 (C=O pyranone), 1570 (C=C). $^1$H NMR ($CDCl_3$) $\delta$/ppm: 8.32 (1H, d, Ar–H), 8.01 (1H, s, H-2), 7.56 (2H, d, Ar–H), 7.45 (2H, d, Ar–H), 7.31 (1H, d, Ar–H), 7.16–7.19 (1H, dd, Ar–H), 2.59–2.64 (2H, t, $CH_2COO$), 1.74–1.82 (2H, m, $C\underline{H}_2$–$CH_2COO$), 1.29–1.45 (12H, m, $CH_3(C\underline{H}_2)_6$–$C_2H_4COO$), 0.87–0.91 (3H, t, $C\underline{H}_3$). $^{13}$C NMR ($CDCl_3$) $\delta$/ppm: 175.58 (C=O pyranone), 171.71 (C=O ester), 157.08, 155.23, 153.36, 132.09, 130.88, 128.19, 125.01, 122.97, 120.09, 117.88, 111.28 ($C_{arom}$), 34.80, 32.21, 29.75, 29.59, 29.44, 25.18, 23.01, and 14.40 ($\underline{C}_9H_{19}COO$–).

**16**: Yield 50%. Analysis: calculated for $C_{26}H_{30}O_4$. C 76.82, H 7.44%; found C 75.96, H 7.54%. IR (KBr)/$cm^{-1}$: 2959, 2925, 2852 ($CH_2$ aliphatic), 1743 (C=O ester), 1647 (C=O pyranone), 1575 (C=C). $^1$H NMR ($CDCl_3$) $\delta$/ppm: 8.35 (1H, d, Ar–H), 8.01 (1H, s, H-2), 7.48 (2H, d, Ar–H), 7.31 (1H, d, Ar–H), 7.28 (2H, d, Ar–H), 7.16–7.19 (1H, dd, Ar–H), 2.61–2.65 (2H, t, $C\underline{H}_2COO$), 2.42 (3H, s, $CH_3$), 1.76–1.84 (2H, m, $C\underline{H}_2$-$CH_2COO$), 1.23–1.49 (12H, m, $CH_3(C\underline{H}_2)_6$–$C_2H_4COO$), 0.89–0.93 (3H, t, $C\underline{H}_3$). $^{13}$C NMR ($CDCl_3$) $\delta$/ppm: 175.71 (C=O pyranone), 171.50

(C=O ester), 156.71, 154.61, 152.88, 138.22, 129.26, 128.83, 128.62, 127.85, 125.54, 122.31, 119.52, 110.90 ($C_{arom}$), 34.44, 31.88, 29.43, 29.27, 29.10, 24.83, 22.69, 14.12 ($\underline{C}_9H_{19}COO$–), and 21.28 (Ar-$CH_3$).

**17**: Yield 50%. Analysis: calculated for $C_{26}H_{30}O_5$. C 73.91, H 7.16%; found C 73.68, H 7.20%. IR (KBr)/$cm^{-1}$: 2952, 2924, 2852 ($CH_2$ aliphatic), 1763 (C=O ester), 1638 (C=O pyranone), 1235 (C–O), 1572 (C=C). $^1$H NMR ($CDCl_3$) $\delta$/ppm: 8.32 (1H, d, Ar–H), 7.98 (1H, s, H-2), 7.50 (2H, d, Ar–H), 7.29 (1H, d, Ar–H), 7.14–7.17 (1H, dd, Ar–H), 6.98 (2H, d, Ar–H), 3.84 (3H, s, $OCH_3$), 2.59–2.63 (2H, t, C$\underline{H}_2$COO), 1.74–1.80 (2H, m, C$\underline{H}_2$-$CH_2$COO), 1.29–1.45 (12H, m, $CH_3(C\underline{H}_2)_6$–$C_2H_4$COO), 0.87–0.91 (3H, t, C$\underline{H}_3$). $^{13}$C NMR ($CDCl_3$) $\delta$/ppm: 175.81 (C=O pyranone), 171.49 (C=O ester), 159.74, 156.68, 154.58, 152.60, 130.13, 127.81, 125.18, 123.84, 122.24, 119.48, 114.04, 110.88 ($C_{arom}$), 55.35 (Ar–$OCH_3$), 34.41, 31.86, 29.41, 29.25, 29.08, 24.81, 22.67, and 14.11 ($\underline{C}_9H_{19}COO$–).

**18**: Yield 50%. Analysis: calculated for $C_{25}H_{28}O_4$. C 76.50, H 7.19%; found C 74.90, H 6.88%. IR (KBr)/$cm^{-1}$: 2953, 2922, 2851 ($CH_2$ aliphatic), 1745 (C=O ester), 1647 (C=O pyranone), 1572 (C=C). $^1$H NMR ($CDCl_3$) $\delta$/ppm: 8.33 (1H, d, $J_{58}$=8.7, H-5), 8.01 (1H, s, H-2), 7.56 (2H, d, Ar–H), 7.39–7.47 (3H, Ar–H), 7.30 (1H, d, Ar–H), 7.16–7.18 (1H, dd, Ar–H), 2.59–2.63 (2H, t, C$\underline{H}_2$COO), 1.74–1.80 (2H, m, C$\underline{H}_2$–$CH_2$COO), 1.29–1.45 (12H, m, $CH_3(C\underline{H}_2)_6$–$C_2H_4$COO), 0.87–0.91 (3H, t, C$\underline{H}_3$). $^{13}$C NMR ($CDCl_3$) $\delta$/ppm: 175.57(C=O pyranone), 171.48 (C=O ester), 156.69, 154.66, 143.15, 131.59, 128.97, 128.54, 128.32, 127.85, 125.60, 122.30, 119.59, 110.92 ($C_{arom}$), 34.42, 31.86, 29.41, 29.25, 29.08, 24.52, 22.68, and 14.12 ($\underline{C}_9H_{19}COO$–).



## 3. Results and discussion

### 3.1. *Thermal and mesomorphic properties*

The phase sequences for compounds **13**–**18** with well-defined transition temperatures are shown in Table 1.

All final compounds, except compound **18**, exhibit enantiotropic properties where the endotherm characteristics of crystal-mesophase-isotropic transitions above melting temperatures were recorded during the heating and cooling runs. Such transitions have also been supported by the enthalpy values of the respective compounds. Observation under crossed polarisers of compounds **13**–**15** with F, Cl, or Br as *para*-substituents show the formation of batonnets that coalesce to form a focal conic fan-shape texture characteristic of SmA, as reported in the literature (*11*). The appearance of SmA is found to agree with earlier reported heterocyclic compounds (*3*).

Figure 1 (a) shows a representative optical photomicrograph of compound **15** exhibiting focal conic fan-shaped texture. Among all the title compounds, only compounds **14** and **17** show the endotherm in the DSC thermogram prior to the crystal-mesophase transition at 85.1 and 68.3°C, respectively (Table 1). The texture observed under a POM has further confirmed the presence of crystalline polymorphism before melting. Compound **16** exhibits smectogenicity with SmA focal conic fan-shaped and nematic schlieren textures (Figure 1 (b)), as well as marble textures (Figure 1 (c)].

Table 1. Transition temperatures and enthalpies for the isoflavonic esters 7-decanoyloxy-3-(4′-substitutedphenyl)-4H-1-benzopyran-4-ones.

| Compound | Transition temperatures/°C(Enthalpy changes/ kJ mol$^{-1}$) upon heating and cooling |
|---|---|
| **13** | Cr 97.5 (31.11) SmA 112.2 (1.07) I<br>I 114.6 (2.11) SmA 109.1 (27.89) Cr |
| **14** | Cr 85.1 (1.42) $Cr_1$ 96.7(22.83) SmA 157.9 (5.50) I<br>I 160.0 (5.46) SmA 111.9 (22.98) $Cr_1$ 86.9 (1.38) Cr |
| **15** | Cr 109.0 (21.41) SmA 165.6 (5.23) I<br>I 167.6 (5.17) SmA 120.0 (21.52) Cr |
| **16** | Cr 70.0 (21.72) SmA 103.8 (1.58) N 111.7(1.43) I<br>I 112.8 (1.15) N 104.9 (1.59) SmA 93.5 (22.37) Cr |
| **17** | Cr 68.3 (2.58) $Cr_1$ 72.7 (21.49) N 114.8 (0.55) I<br>I 117.1 (0.49) N 93.9 (24.86) Cr |
| **18** | Cr 73.2 (36.30) I<br>I 92.8 (35.46) Cr |

Inspection of Figure 2 shows a broad peak with relatively low intensity at 110.0°C. This observation can be due to a poor scattering from the molecules in the N phase. The X-ray pattern as observed at the same temperature (Figure 3) shows two diffuse peaks, which could result from the disordered molecular arrangement. The *d*-spacing at this temperature at low angles $2\theta$=3.39° is found to be 24.7 Å. This measurement is in accordance with the molecular distance measured in a monocrystal (24.0 Å). Therefore, it can be deduced that on average the long molecular axis of compound **16** is pointing in one favorable direction with a small interaction coefficient.

It can also be observed from Figure 2 that upon cooling of compound **16**, a transition from the N to SmA phase shows a sharp peak with high intensity corresponding to a strong scattering from the molecules at 90.0°C. The two diffused signals as recorded in N phase become very sharp (Figure 4).

Compound **17**, on the other hand, shows only a nematic phase and the texture at the clearing temperature is typical of the nematic-isotropic transition. Compound **18** is the only non-mesogenic compound within this series in which the molecular

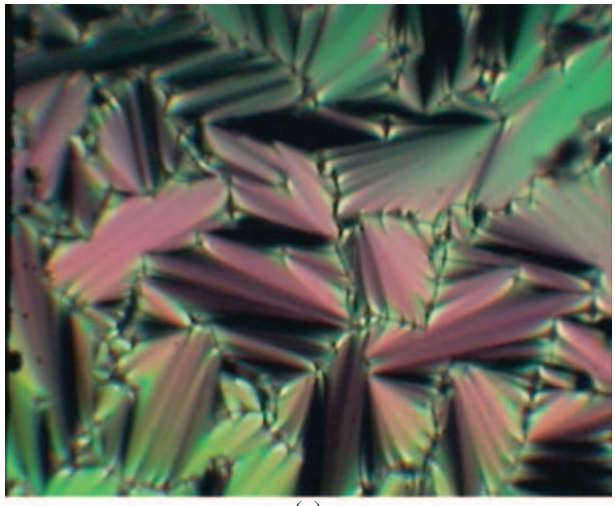

(a)

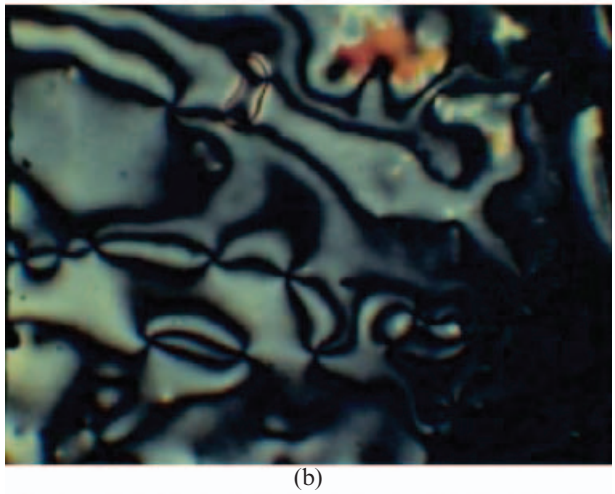

(b)

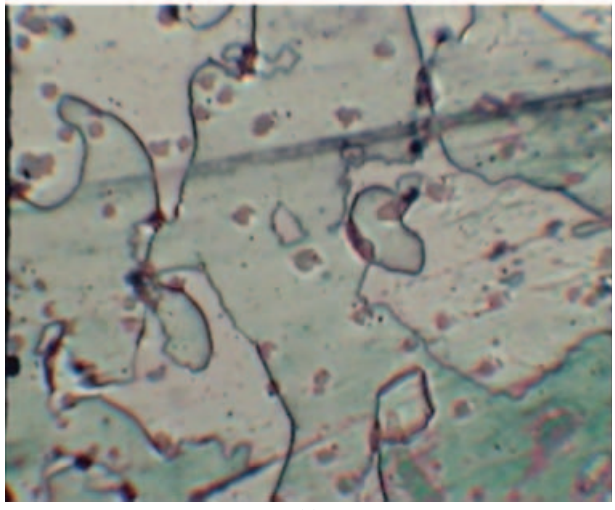

(c)

Figure 1. (a) Optical photomicrograph of compound **15** displaying focal conic fan-shaped of SmA; (b) and (c) optical photomicrographs showing schlieren (upon heating) and marble (upon cooling) textures for compound **16**.

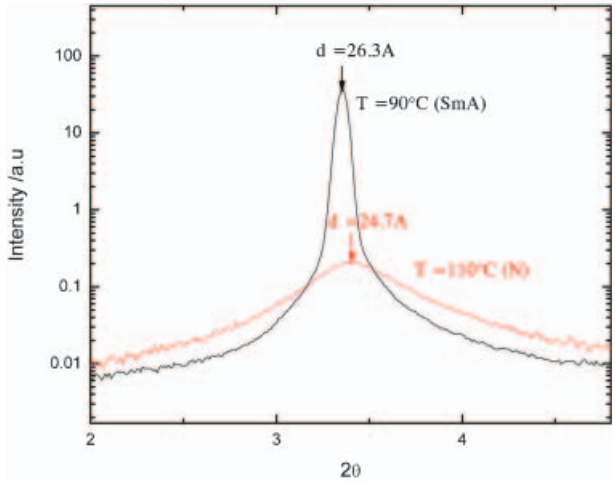


Figure 2. The XRD pattern and the one-dimensional intensity versus $2\theta$ profiles for compound **16** in N (110°C) and SmA (90°C) phases during a cooling mode.

arrangement is not favourable for the mesophase formation. All the title compounds except compound **15** possess melting temperatures below 100°C. This phenomenon can probably be explained in terms of the polarisability of the molecules, as discussed in the following section.

### 3.2. *Correlation between the mesomorphic properties and structural changes*

The calculated polarisability values are tabulated in Table 2. Since the long-range orientational order of

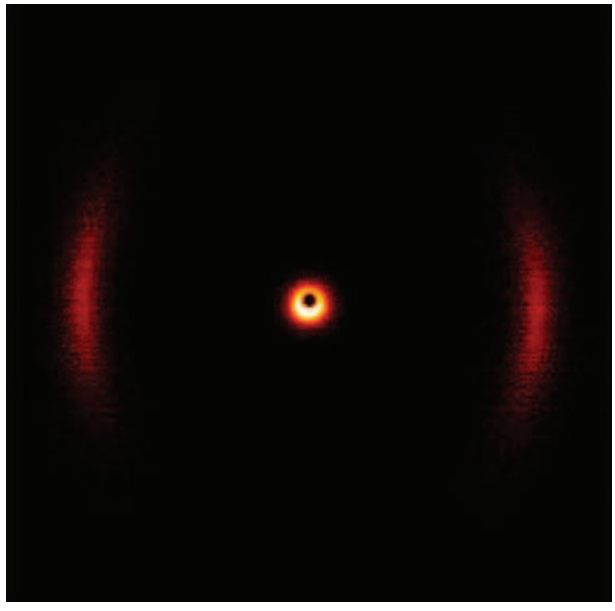

Figure 3. An X-ray diagram of compound **16** in N phase at 110.0°C upon cooling. The two signals observed in SmA phase become diffused due to a loss in lamellar arrangement of molecules in the N phase.

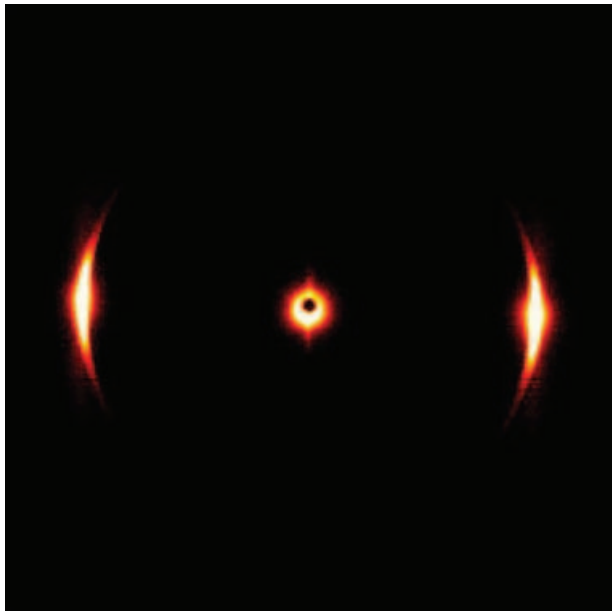

Figure 4. An X-ray diagram of compound **16** in SmA phase at 90.0°C upon cooling. The molecules are aligned in the magnetic field. The two sharp signals indicate a lamellar arrangement of molecules.



the molecules can be ascribed to the anisotropic dispersion force alone, it suggests that a linear relationship between the clearing temperatures and polarisability anisotropy of the $C_{Ar}$–X bond must exist. However, the inspection of DSC data shows that not all the title compounds exhibit this relationship, since the mesomorphic properties of a compound is a consequence of the balance between the attractive (owing to the molecular polarisability and polarity) and repulsive (essentially governed by the steric factor) forces (*12*).

In addition to the polarisability factor, the influence of different substituent R is also a contributing factor to the difference in clearing temperatures of title compounds. From DSC thermograms for compounds **13**–**15** with different substituent R at *para* position, compound **13** shows a clearing temperature very much lower than those of compounds **14** and **15**. This observation suggests that the valence electrons of F, the most electronegative atom from Group 17, are tightly held to its nucleus resulting in a low polarisability. As a result, it reduces the degree of molecular order. Conversely, the Cl and Br atoms with larger radii and loosely held valence electrons are relatively easy to polarise (*13*). The steric effect associated with the asymmetry of the central core as well as the molecular size of the substituent R is the least in the compound bearing the F atom, compared to the compounds with Cl and Br atoms. Consequently, the clearing temperatures for the title compounds bearing R=F, Cl, or Br will increase in the order of F>Cl>Br. This is confirmed by the calculated polarisability values, as shown in Table 2.

Table 2. Calculated polarisability values for compounds **13**–**18**.

| Compound | Polarisability ($\alpha \pm 0.5 \times 10^{-24}$) |
|---|---|
| **13** | 44.63 |
| **14** | 46.58 |
| **15** | 47.69 |
| **16** | 46.55 |
| **17** | 47.28 |
| **18** | – |

Another noticeable feature is that the nematic-isotropic transition temperature of compound **17** was slightly higher than that of compound **16**. This observation can be explained in terms of the presence of an O atom from the methoxy group in compound **17**, which enhances the polarisability apart from extending the length of the rigid central core. This reasoning is also in accordance with the calculated polarisability (Table 2).

### 3.3. *Physical characterization*

#### *3.3.1. FT-IR spectral studies.*

The FT-IR spectra of compounds **1**–**6** show the absorption bands assignable to the stretching of OH at 3137–3419 $cm^{-1}$. Bands appearing within the frequency range of 2836–2922 $cm^{-1}$ can be ascribed to the stretching of aliphatic C–H. Whilst the stretching of C=O (ketone) appears at 1623–1639 $cm^{-1}$, the signal ascribed to the C=C aromatic is observed at 1549–1598 $cm^{-1}$. An additional band attributable to the stretching of C–O is observed for compound **5** at 1244 $cm^{-1}$. Two of the earlier mentioned bands corresponding with the stretching of C–H and C=O (ketone) are absent in compounds **7**–**12**. Instead, the stretching of C=O (pyranone) at 1630–1647 $cm^{-1}$ is recorded. Compounds **13**–**18**, on the other hand, show bands at 2851–2959, 1742–1763, 1637–1648, and 1609–1570 $cm^{-1}$, which can be assigned to the stretching of aliphatic C-H, C=O ester, C=O pyranone, and C=C, respectively. An absorption occurring at 1235 $cm^{-1}$ can be attributed to the stretching of C–O in compound **17**.

#### *3.3.2. $^{1}H$ and $^{13}C$ NMR spectral studies.*

The $^{1}H$ NMR spectra of compounds **1**–**12** show the singlet and multiplet at respective chemical shifts of $\delta$=9.56–12.75 ppm and $\delta$=6.32–8.54 ppm, which can be assigned to the hydroxyl (OH) and aromatic protons. The presence of methylene ($CH_2$) protons in

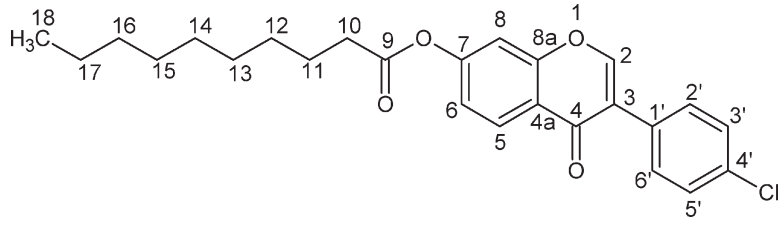


Figure 5. Atomic numbering scheme in relation to NMR assignment for compound **14**.

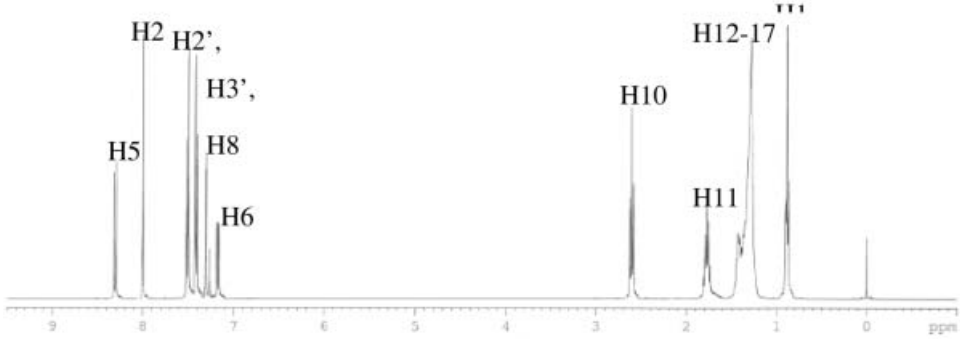


Figure 6. $^{1}$H NMR spectrum and structural assignment of compound **14**.



compounds **1**–**6** is observed as a singlet at $\delta$=4.23–4.35 ppm. The compounds **4**, **5**, **10**, and **11** show an additional peak attributable to the presence of methyl protons at $\delta$=2.28, 3.77, 3.48, and 3.45 ppm, respectively. The $^{1}$H NMR spectra for compounds **13**–**18**, on the other hand, show the presence of seven aromatic protons with variable multiplicities within the range of $\delta$=7.12–8.43 ppm. The two separate triplets assignable to the methyl group at the ester linkage and $CH_2$–COO protons are observed at $\delta$=0.87–0.91 and 2.59–2.64 ppm, respectively. Multiplets at $\delta$=1.29–1.45 and 1.69–1.82 ppm can be assigned to the methylene protons in the respective $C\underline{H}_2$–$CH_2$–COO and $CH_3$–$(C\underline{H}_2)_7$–$CH_2$–COO fragments. The additional signal ($\delta$=2.42 and 3.84), as in the $^{1}$H NMR spectra for compounds **16** and **17**, can substantiate the presence of Ar-$CH_3$ and Ar-$OCH_3$ in respective compounds **16** and **17**. The presence of different substituents, R (where R=F, Cl, Br, $CH_3$, $OCH_3$, or H) in compounds **13**–**18** has led to different

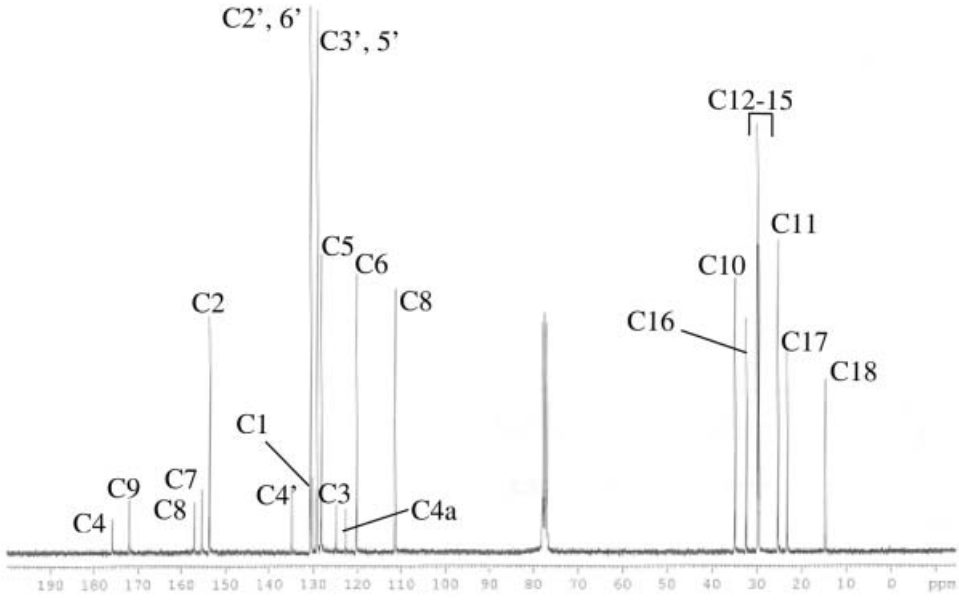


Figure 7. $^{13}$C NMR spectrum and structural assignment of compound **14**.

chemical shifts as well as the splitting of the aromatic protons. $^{13}C$ NMR spectroscopy is used to further substantiate the molecular structures of the title compounds. A complete structural assignment of compounds **13–18** has been carried out with the aid of DEPT and two-dimensional $^{1}H$-$^{1}H$ COSY, HMQC, and HMBC experiments. Compound **14** is selected as a representative for further illustration.

The atomic numbering scheme in relation to the NMR spectra for compound **14** is shown in Figure 5. The representative spectra of $^{1}H$ and $^{13}C$ NMR for compound **14** are depicted in Figures 6 and 7, respectively. The results as inferred from the IR and NMR spectral data of all compounds are found to be consistent with the proposed structure, as shown in Scheme 1.

**Acknowledgement**

The main author, G-Y. Yeap, would like to thank Universiti Sains Malaysia and the Malaysian Government, especially the Ministry of Science, Technology and Innovation (MOSTI), for the eScience Fund (Grant No. 305/PKIMIA/613315) and USM Short-Term (Grant No. 304/PKIMIA/636103).



**References**

(1) Chudgar N.K.; Paresh M.K.; Madhavrao S.S.; Sharma H.C. *Liq. Cryst.* **1995**, *19*, 807–810.
(2) Hirose T.; Tsuya K.; Nihigaki T.; Idaka E.; Yano S. *Liq. Cryst.* **1989**, *4*, 653–659.
(3) Belmar J.; Parra M.; Zuniga C.; Perez C.; Munoz C. *Liq. Cryst.* **1999**, *26*, 75–81.
(4) Yeap G.Y.; Yam W.S.; Ito M.M.; Takahashi Y.; Nakamura Y.; Mahmood W.A.K.; Boey P.L.; Hamid S.A.; Gorecka E. *Liq. Cryst.* **2007**, *34*, 649–654.
(5) Bruker Program ID WIN-NMR (release 6.0) and 2D WIN-NMR (release 6.1). Bruker Daltonik GMBH, Bremen, Germany.
(6) Yeap G.Y.; Ha S.T.; Nakamura Y.; Boey P.L.; Mahmood W.A.K.; Ito M.M.; Nakai H.; Yamaki M. *Spect. Lett.* **2004**, *37*, 319–336.
(7) Yeap G.Y.; Ha S.T.; Ito M.M.; Boey P.L.; Mahmood W.A.K. *J. Mol. Struct.* **2004**, *687*, 57–64.
(8) Pelter A.; Ward R.S.; Gray T.I. *J. Chem. Soc. Perkin I* **1976**, 2475–2479.
(9) Wahala K.; Hase T.A. *J. Chem. Soc. Perkin Trans I* **1991**, 3005–3008.
(10) Bass R.J. *J. Chem. Soc. Chem. Comm.* **1976**, 78–79.
(11) Demus D.; Richter L. *Textures of Liquid Crystals*, New York: Verlag Chemie, **1978**, 11–83.
(12) Barbera J.; Marcos M.; Ros M.B.; Serrano J.L. *Mol. Cryst. Liq. Cryst.* **1988**, *163*, 139–155.
(13) Solomons T.W.G. *Fundamentals of organic Chemistry*, New York: Wiley, **1994**, 11–15.